Talanta 130 (2014) 408–414

Contents lists available at ScienceDirect

Talanta

journal homepage: www.elsevier.com/locate/talanta

One-step facile synthesis of hyaluronic acid functionalized fluorescent gold nanoprobes sensitive to hyaluronidase in urine specimen from bladder cancer patients

Dan Cheng [a], Weiye Han [a], Kuncheng Yang [a], Yang Song [a], Mingdong Jiang [b], Erqun Song [a,*]

[a] Key Laboratory of Luminescence and Real-Time Analytical Chemistry (Southwest University), Ministry of Education, College of Pharmaceutical Sciences, Southwest University, Chongqing 400715, China
[b] Department of Oncology, The Ninth People's Hospital of Chongqing, Chongqing 400700, China

ARTICLE INFO

Article history:
Received 31 March 2014
Received in revised form
28 June 2014
Accepted 2 July 2014
Available online 10 July 2014

Keywords:
Gold nanoparticle
Fluorescence resonance energy transfer
Hyaluronic acid
Hyaluronidase
Nanoprobe
Tumor

ABSTRACT

Gold nanoparticles (AuNPs) have been widely used to develop fluorescence resonance energy transfer (FRET) sensors to detect biological substances, environmental pollutants, and disease markers due to their superior quenching capacity to fluorescence signals. In this study, we report the one-step facile synthesis of fluorescein isothiocyanate-labeled hyaluronic acid (FITC–HA) functionalized fluorescent AuNPs based FRET nanoprobes (FITC–HA–AuNPs) *via* chemical reduction of $HAuCl_4$ by using FITC–HA as both a reducing and stabilizing agent. Then the FITC–HA–AuNPs FRET nanoprobes were used to detect hyaluronidase (HAase), a new type of disease marker, based on the specific enzymatic degradation of HAase to HA. Compared with similar work, the FITC–HA–AuNPs nanoprobes were much easier to prepare and the detection sensitivity was also high for HAase to reach a detection limit of 0.63 U mL^{-1}. More importantly, they also allowed for rapid HAase detection (within 3 h) even in complex biological specimens (urine specimens from patients with bladder cancer) with satisfactory accuracy (recovery efficiency in the range of 92.8–106.9% with RSD $\leq$ 4.85%). Our studies suggested that such a novel design of FITC–HA–AuNPs FRET nanoprobes developed for sensitive, rapid and accurate detection of HAase had exciting potentials for clinical diagnosis of HAase-related diseases, such as bladder cancer.

1. Introduction

Recent studies have showed that hyaluronic acid (HA) and hyaluronidase (HAase) had a close relationship with the proliferation, differentiation, migration, and adhesion of tumor cell and the tumor angiogenesis based on the highly efficient targeted delivery tumor cell with HA receptors such as hyaluronan receptor for endocytosis (HARE) and cluster determinant 44 (CD44) [1–3], and they have played an important role in tumor invasion, metastasis and progression [4,5]. HA is a macromolecule of linear polysaccharide, composed of repeating disaccharide units, D-glucuronic acid and N-acetyl-D-glucosamine, with good water solubility [6]. The HAase is an enzyme that degrades HA specifically by cleaving the internal β-N-acetyl-D-glucosamine linkages in the HA polymer, thereby increasing the tissue permeability [7]. As HAase had been reported to over express in certain patients with cancers (such as bladder, colon, prostate, and so on), it is becoming a new type of tumor marker [7–9]. Therefore, it will be of great significance to develop simple, rapid, and sensitive methods for detection of HAase. There are various strategies for HAase detection including turbidimetric [10,11], viscometric [12], zymography [13], immunoassay[14,15], instrument [16,17], and chemical methods such as colorimetric method [18–20], spectrophotometric [21], fluorescence detection [22–24], and chemiluminescence-assisted assay [25]. Among the strategies for HAase assay, the classical methods (turbidimetric, viscosimetric and colorimetric methods) often lack sensitivity and selectivity [26]. Zymography method is simple but not suitable for sensitive quantitative analysis. Immunoassay is sensitive and selective but needs specialized and expensive reagents (anti-HAase antibodies). And instrument-based method is sensitive and accurate but time-consuming and requires complex instruments. Thus, developing new precise and accurate methods for HAase assay is needed.

Fluorescence resonance energy transfer (FRET) is a powerful analytical technique, which has been widely used for target detection and molecular interaction study because of its high sensitivity, specificity and simplification [27]. Recently, this analysis method has been developed and improved largely due to the rapid development of new materials, especially nanomaterials such as quantum dots [28], carbon dots [29], AuNPs [30], carbon

* Corresponding author. Tel./fax: +86 2368251225.
E-mail address: eqsong@swu.edu.cn (E. Song).

http://dx.doi.org/10.1016/j.talanta.2014.07.005
0039-9140/

nanotubes [31], graphene [32,33]. The nanomaterial-based FRET analytical technique not only breaks the detection distance limitation that the traditional fluorescent dye-based FRET technique requires (the distance between donor and receptor should be within 10 nm), but also improves the sensitivity and broads its applications [34]. Among the new nanomaterials, AuNPs is a kind of efficient fluorescence quencher because of the non-radioactive electronic excitation energy transfer from the fluorophore to AuNPs [35]. They also have many other advantages such as simple synthesis, facile surface modification, tunable optical properties and good stability [36]. Therefore, AuNPs have been widely used to construct FRET probes for the detection of various ions, small molecules, biomolecules, and pathogens [37–39].

Based on the above-mentioned knowledge, we can envision that it must be a very interesting work to development a new method for the detection of HAase by combining the property of degradation of HAase to HA with AuNPs-based FRET analytical technique. Currently, there are very few reports about the detection of HAase by using AuNPs based FRET nanoprobes. Lee et al. made some attempts in fabricating AuNPs FRET nanoprobes by assembling dye-labeled HA onto the pre-prepared AuNPs surface based on gold–thiol bond covalent interaction, and applying the probes for HAase detection by the specific enzymatic degradation of HAase to HA [40]. However their work involves complicated procedure for preparation of AuNPs FRET probes, resulting time-consuming, and is lack of analysis for clinical specimens.

Previously, we had successfully developed N-acetylglucosamine-functionalized AuNPs by using polysaccharide as a ligand [41]. Herein, as a further step, by employing fluorescein isothiocyanate-labeled hyaluronic acid (FITC–HA) as both a reducer and stabilizer to deoxidize chloroauric acid ($HAuCl_4$), we have prepared FITC–HA functionalized fluorescent AuNPs (FITC–HA–AuNPs) as FRET nanoprobes in one step in a facile manner. The resultant FITC–HA–AuNPs FRET nanoprobes are of uniform size and good stability, which are subsequently used to develop a simple, rapid, and sensitive strategy for detection of HAase in urine specimens from patients with bladder cancer (Scheme 1). Compared with similar work [40], our work not only simplifies the preparation procedure of AuNPs FRET probes, but also improves the detection limit (as low as 0.625 U mL^{-1}) for HAase analysis. Moreover, the AuNPs FRET nanoprobes could detect HAase in clinical specimens (urine specimens from patients with bladder carcinoma) directly with good accuracy within 3 h, which is the first report to the best of our knowledge. Such FITC–HA–AuNPs FRET nanoprobes show promising potential for clinical diagnosis of HAase-related diseases.

2. Experimental

2.1. Instrumentations

The fluorescence spectra were obtained using a fluorescence spectrophotometer (F-7000, Hitachi). UV–vis absorption spectra were recorded by a UV–vis spectrophotometer (UV-2450, Shimadzu). Morphology and microscopic structure were characterized using a transmission electron microscope (TEM) (LIBRA 200PE, German Carl Zeiss Company). Size distribution was recorded by Zetasizer Nano ZS (Malvern Instruments Ltd.).

2.2. Standard solutions and reagents

Fluorescein hyaluronic acid (FITC–HA) and hyaluronidase (HAase) were purchased from Sigma-Aldrich Co. Ltd.; sodium citrate was obtained from Chongqing Chuandong Chemical Co. Ltd.(China); chloroauric acid ($HAuCl_4$) was provided by Tianjin Guangfu Chemical Research Institute; human serum albumin (HSA) was purchased from Beijing Dingguo biotechnology Co. Ltd.; carbamide, uric acid, creatinine, benzoylglycine were obtained from Sinopharm Chemical Reagent Co., Ltd.; human serum (HS) and human urine specimens were supported by Department of Oncology, the Ninth People's Hospital of Chongqing (China); all the buffers were prepared with double-distilled water which was purified with a water purification system (ELGA, British) to a specific resistance of 18 MΩ cm.

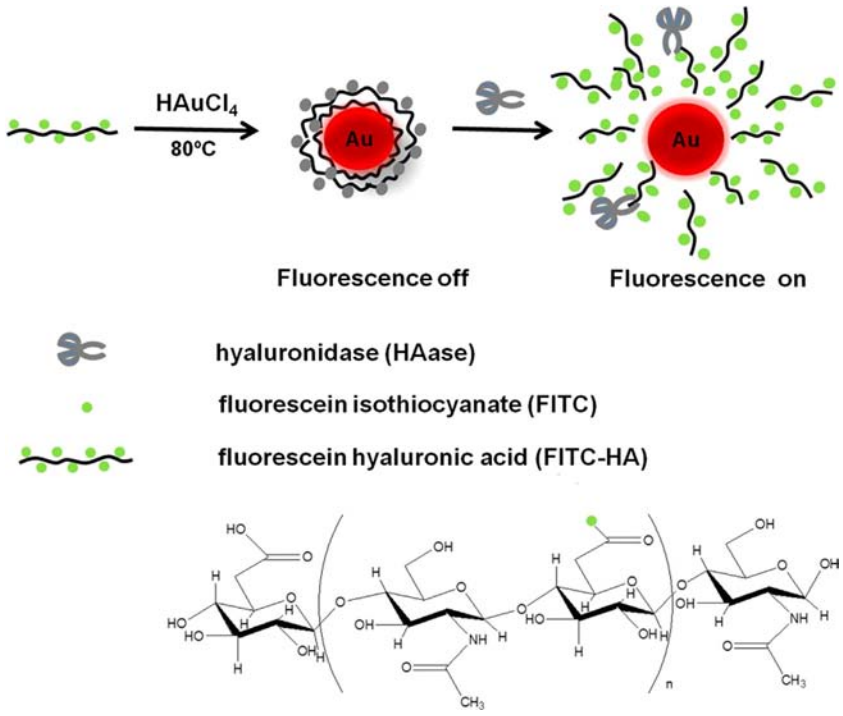

Scheme 1. Schematic illustration of the one-step synthesis of FITC–HA–AuNPs nanoprobes and their application as optical nanoprobes for HAase detection.

2.3. Synthesis of FITC–HA–AuNPs

The FITC–HA–AuNPs were synthesized according to our previous work with some modifications [41]. In a typical synthetic procedure, 2.00 mg (2.5 nmol) of FITC–HA was dissolved in 1.5 mL of 0.01 mol L^{-1} phosphate buffer solution (NaH_2PO_4, Na_2HPO_4, pH 7.4) (PB) in a bottle under stirring, and the mixture was slowly heated to 60 °C. Then, 50 μL of 1% (W/V) $HAuCl_4$ aqueous solution was added dropwise to the above solution. The solution was gradually heated to 80 °C until the solution color changed to pink. After cooled down to room temperature, the product was stored at 4 °C in the dark.

2.4. Stability of FITC–HA–AuNPs nanoprobes

The effect of different buffer solutions on the stability of FITC–HA–AuNPs nanoprobes was studied. FITC–HA–AuNPs and citrate–AuNPs were respectively treated with Britton–Robison buffer (BR buffer) solution with pH 2.0 and 12.0, NaCl (1.0 M) solution, and 10% HS. The color of the solutions was recorded using a digital camera after 30 min.

The storage stability of FITC–HA–AuNPs nanoprobes was further investigated upon storage by measuring the fluorescence signals *vs*. various times of storage.

2.5. Detection of HAase with FITC–HA–AuNPs nanoprobes

HAase solutions with different concentrations were incubated with the FITC–HA–AuNPs nanoprobes (60 nM) for 3 h at 37 °C in 0.01 M PB (pH 7.4) in the dark [40], followed by recording the fluorescence intensity of the solution. The fluorescence intensity of each specimen was recorded at $\lambda_{ex/em}$=480/520 nm.

2.6. Determination of HAase in urine specimens with FITC–HA–AuNPs nanoprobes

Human urine specimens from five healthy people and five patients with bladder carcinoma were centrifugated at 4000g/10 min firstly [20]. Prior to analysis, the urine specimens from patients with bladder carcinoma were diluted 10 times to ensure that the concentrations of HAase were in the linear range of the assay done above. Then, the concentrations of HAase in urine specimens were determined by using FITC–HA–AuNPs nanoprobes according to the same procedure as described above.

3. Results and discussion

3.1. Synthesis of FITC–HA–AuNPs

In order to obtain FITC–HA–AuNPs nanoprobes with high quality, their synthesis conditions were optimized. It is known that the amount of $HAuCl_4$ had an important effect on the quality of FITC–HA–AuNPs, and on the other hand, the stability of FITC–HA is related to the ambient temperature based on the published work [42]. Therefore, in the present study the molar ratio of FITC–HA to $HAuCl_4$ ($n_{FITC-HA}$:n_{HAuCl4}) and the reaction temperature were mainly investigated when preparing FITC–HA–AuNPs nanoprobes. First, at the reaction temperature of 80 °C, the effect of different $n_{FITC-HA}$:n_{HAuCl4} (1:240; 1:480; 1:960) on the quality of product was studied. As shown in Fig. 1A, the product with golden yellow color and a strong absorption peak at 490 nm (from FITC–HA) was obtained when $n_{FITC-HA}$:n_{HAuCl4} came to 1:240, suggesting a very low yield of FITC–HA–AuNPs nanoprobes at this synthesis condition. And when $n_{FITC-HA}$:n_{HAuCl4} increased to 1:480, the color of product is wine red and a strong absorption at 512 nm was appeared (Fig. 1A), suggesting that a lot of FITC–HA–AuNPs nanoprobes were produced under this condition. However, a purple solution with aggregation was obtained when $n_{FITC-HA}$:n_{HAuCl4} came to 1:960, resulting in an obvious shift of their UV–vis spectra (Fig. 1A).

Next, the effect of reaction temperature on the quality of FITC–HA–AuNPs was investigated. Generally speaking, a higher reaction temperature could speed up the reaction rate. However, on the other hand, HA could be degraded if the ambient temperature was higher than 90 °C [43]. Therefore, two different reaction temperatures of 60 °C and 80 °C were chosed to investigate their effect on the yield of FITC–HA–AuNPs. Results from Fig. 1B showed that there was only a strong absorption at 512 nm from AuNPs for the product obtained at 80 °C while there was still a obvious absorption peak of FITC–HA (at 490 nm) for the product obtained at 60 °C although both of the products appeared with wine red color. These results suggested that the yield of FITC–HA–AuNPs was higher at 80 °C than at 60 °C. And what is interesting is that the product synthesized in the condition of $n_{FITC-HA}$:n_{HAuCl4}=1:480 and $n_{FITC-HA}$:n_{HAuCl4}=1:960 at 80 °C showed much lower backgroud fluorescence signal at the wavelength of 520 nm than other products (as shown in Fig. S1). However, the latter (which produced in conditionn of $n_{FITC-HA}$:n_{HAuCl4}=1:960 at 80 °C) showed obvious aggregation on both the physical digital photo (Fig. 1A) and TEM image (Fig. S2).

Moreover, the absorption spectra form Fig. 1C demonstrated that there was no obvious effect of reaction time on the yield of FITC–HA–AuNPs. Based on the above study, all the FITC–HA–AuNPs used in this work were synthesized with $n_{FITC-HA}$:n_{HAuCl4} for 1:480 at 80 °C for 15 min.

3.2. Characterization of FITC–HA–AuNPs

3.2.1. Morphology and size of FITC–HA–AuNPs

The formation of FITC–HA–AuNPs was confirmed by TEM. TEM micrograph showed that the FITC–HA–AuNPs were uniformed spherical and monodisperse with diameter in the range of 6.0 ± 0.7 nm (Fig. 2A). Dynamic light scattering (DLS) result showed that the average hydrodynamic diameter of FITC–HA–AuNPs were around 9 nm (Fig. 2B). This discrepancy of particle size measured by DLS and TEM is frequently observed when a hydrophilic moiety is coated on a nanoparticle surface [44]. For FITC–HA–AuNPs, the hydrophilic coating of FITC–HA causes an increase in the average hydrodynamic diameter.

3.2.2. Optical characterization of FITC–HA–AuNPs

As FRET probes, their optical properties are important parameters. Fig. 3A showed that FITC–HA–AuNPs have strong absorption at 512 nm. The concentration of FITC–HA–AuNPs was estimated by a reported procedure [45] and the number of FITC–HA moieties on each AuNP was roughly determined by dividing the total molar amount of FITC–HA–AuNPs with the total molar amount of FITC–HA used in the reaction. The result revealed that roughly 5–6 FITC–HA molecules were surface immobilized per AuNP.

The fluorescence spectrum of FITC–HA–AuNPs nanoprobes was shown in Fig. 3B(a2). It could be found that there is almost no any fluorescence signal at the wavelength of 520 nm compared with the pure FITC–HA (Fig. 3B(a1)). This intensive fluorescence quench should be attributed to large absorption of the resultant AuNPs since there is no other quencher in the system. Moreover, the fluorescence spectrum also demonstrated that the as-prepared FITC–HA–AuNPs FRET probes had negligible background signal which was benefit for promoting the sensitivity when applied for assay.

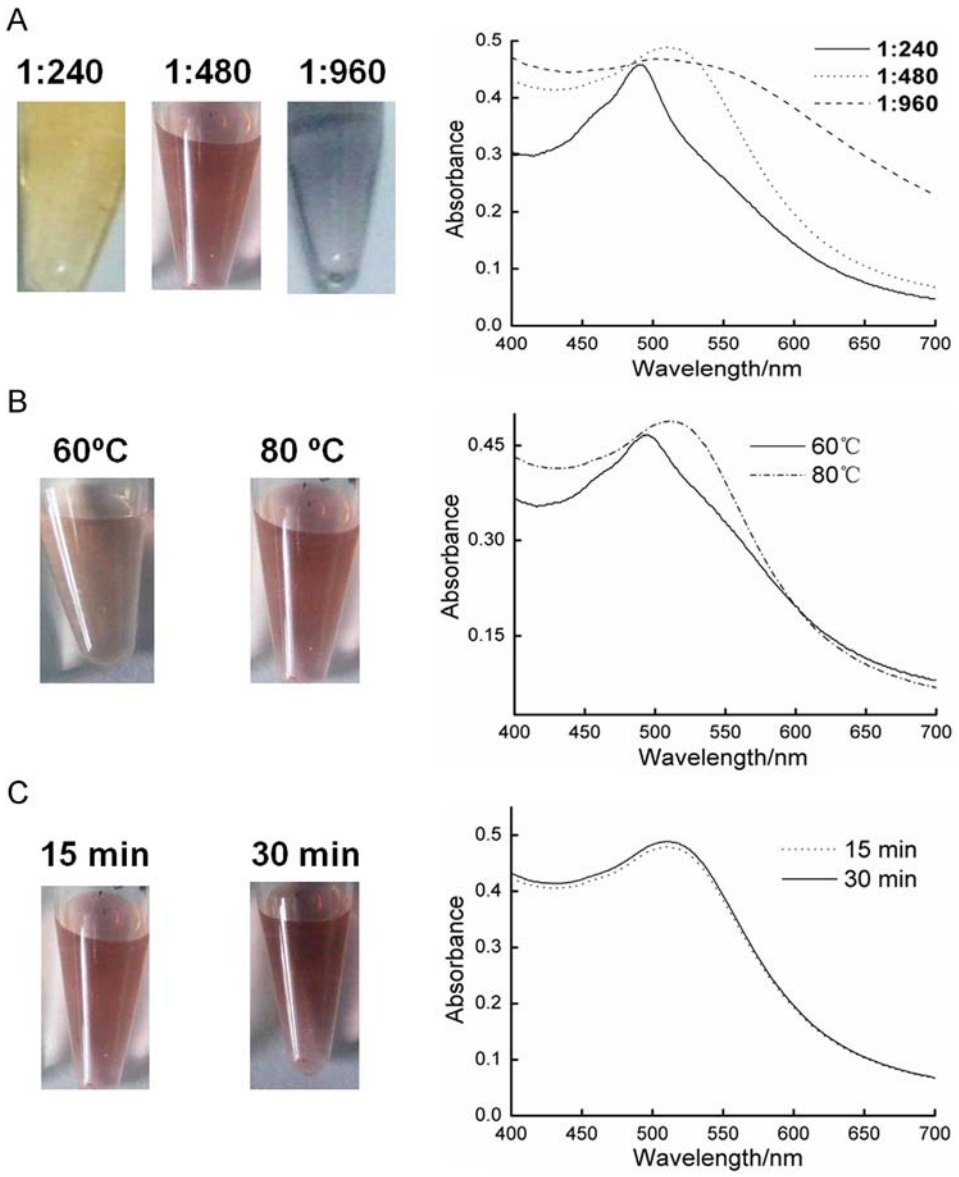

Fig. 1. Photographs and absorption spectra of FITC–HA–AuNPs products under different synthesis conditions. (For interpretation of the references to color in this figure, the reader is referred to the web version of this article.)

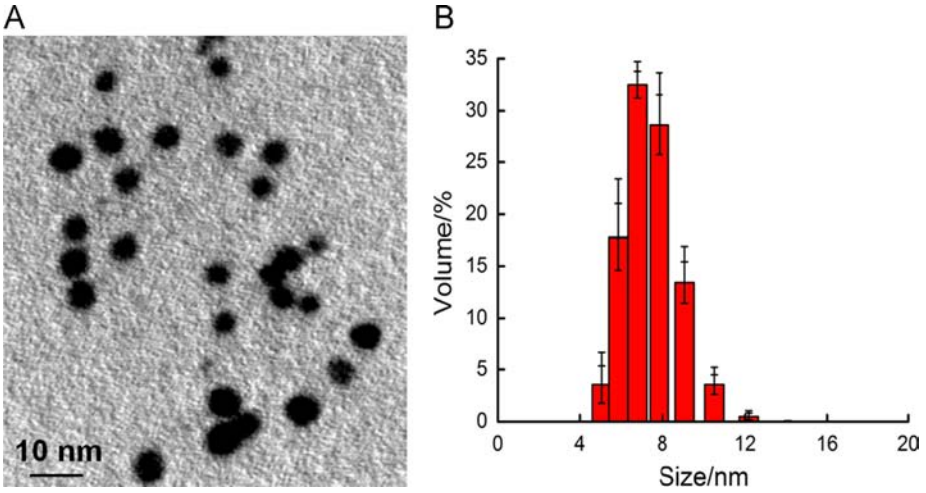

Fig. 2. TEM image (A) and DLS size distribution (B) of FITC–HA–AuNPs.

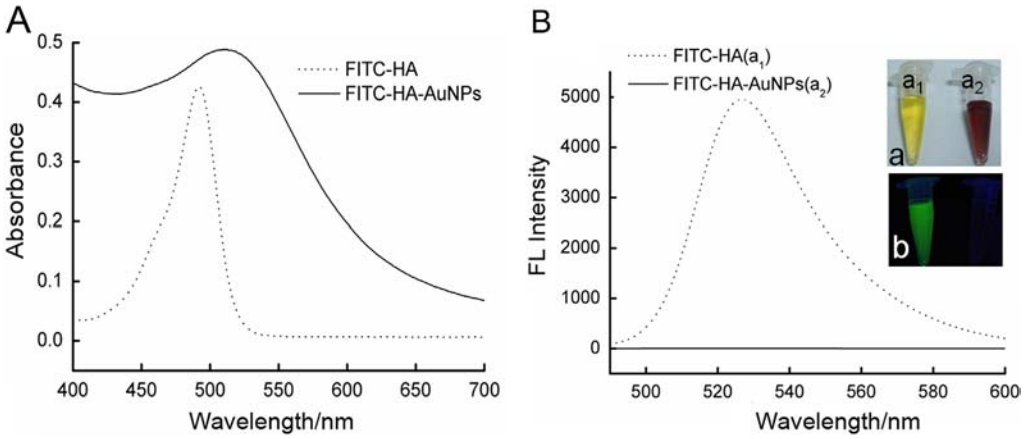

Fig. 3. Absorption (A) and fluorescence spectra (B) of FITC–HA and FITC–HA–AuNPs. Inset shows the photograph of FITC–HA (a_1) and FITC–HA–AuNPs (a_2) under natural (a) and UV (b) light.

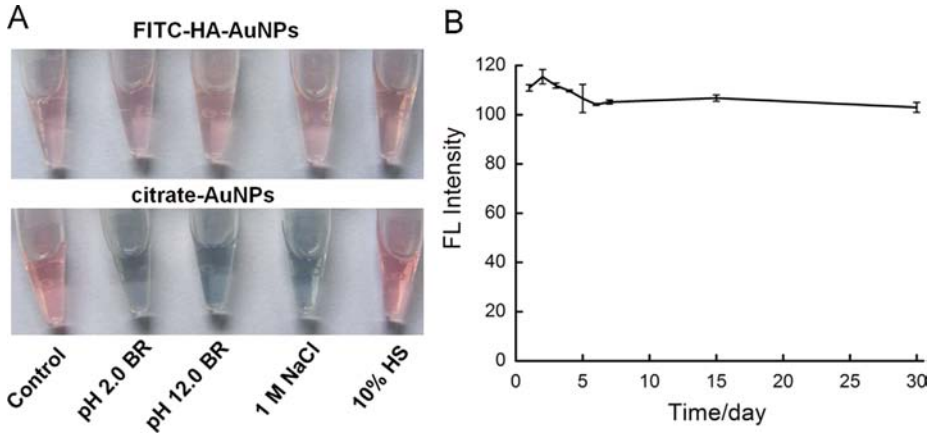

Fig. 4. Stability comparisons of FITC–HA–AuNPs and citrate–AuNPs (A) and fluorescence intensity of FITC–HA–AuNPs *vs.* the storage time (B).

3.2.3. *Zeta potential of FITC–HA–AuNPs nanoprobes*

Zeta potential was measured using Malvern Zetasizer Nano ZS. The zeta potential was -31.4 ± 1.2 mV for FITC–HA–AuNPs, which provided enough surface charge to stabilize the nanoprobes from aggregation.

3.3. *Stability of FITC–HA–AuNPs nanoprobes*

The resultant FITC–HA–AuNPs were very stable. There is no any aggregation of FITC-HA-AuNPs when dispersed in BR buffer with pH values of 2 and 12, in NaCl solution (1.0 M), and also in 10% HS solution (Fig. 4A). In the case of citrate–AuNPs, they tended to instantaneous aggregation under the same condition.

As a nanoprobe, the storage stability is a very important feature for biomedical applications. The stability of FITC–HA–AuNPs nanoprobes was further investigated upon storage by measuring the fluorescence signals along with the storage time. As shown in Fig. 4B, the fluorescence intensity showed negligible change after 30-days storage in aqueous solution at 4 °C in the dark. Such storage stability together with the resistance to pH variation, high salt buffer and other environmental changes supports the potential application of the FITC–HA–AuNPs nanoprobes for the analysis of complex biomedical specimens.

3.4. *Detection of HAase using FITC–HA–AuNPs nanoprobes*

As their stability was proved, the ability of FITC–HA–AuNPs nanoprobes for detecting HAase was further tested. As mentioned above, the HA can be cleaved by HAase, releasing signal probes (FITC) from AuNPs. This will lead to the recovery of the fluorescence intensity of FITC and the HAase can thus be detected based on the increased fluorescence intensity (Scheme 1). Then the FITC–HA–AuNPs nanoprobes were applied to detect HAase.

The assay conditions including reaction buffer, concentration of nanoprobe, and reaction time were optimized and shown in Figs. S3–S5. Later on, a series of HAase solutions with different concentrations (0, 1.25, 2.5, 5, 12.5, 25, 37.5, 50, 62.5, 75 and 125 U mL^{-1}) were incubated with the FITC–HA–AuNPs nanoprobes at 37 °C in the dark for 3 h, followed by the determination of the fluorescence intensity of each specimen. As shown in Fig. 5, the fluorescence intensity increased with increasing amount of HAase. Moreover, the enhanced fluorescence intensity ΔF ($\Delta F = F - F_0$, F and F_0 stands for the fluorescence intensity of FITC–HA–AuNPs nanoprobes after and before reacting with HAase, respectively) was linearly correlated with the concentration of the HAase in the range of 1.25–50 U mL^{-1}. The detection limit of HAase is 0.625 U mL^{-1}, which represents a lower detection limit compared with the previous work [40]. Another several hours later after incubating with HAase for 3 h, the FITC–HA–AuNPs nanoprobes were found to become purple aggregation casually (Fig. S6), which may attribute to the fall-off of HA (after digested by HAase) from the surface of AuNPs resulting less protecting ligands for the AuNPs.

3.5. *Selectivity of FITC–HA–AuNPs nanoprobes for HAase*

Since urine contains complex components, including saline, saccharine, carbamide, uric acid, creatinine, benzoylglycine and

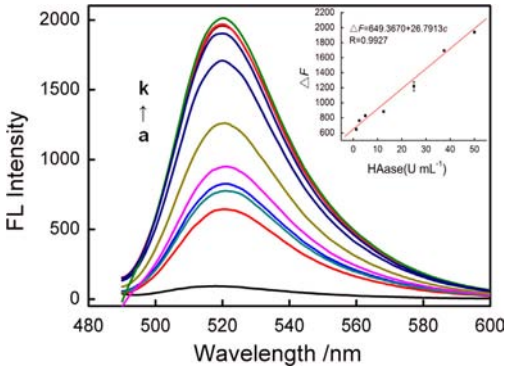

Fig. 5. Fluorescence spectra of FITC–HA–AuNPs solution correlates with HAase concentrations with different concentrations (a–k: 0, 1.25, 2.5, 5, 12.5, 25, 37.5, 50, 62.5, 75 and 125 U mL^{-1}). The inset at the top right indicates the linear regression of the enhanced fluorescence intensity (ΔF, at 520 nm) *vs.* the concentration of HAase.

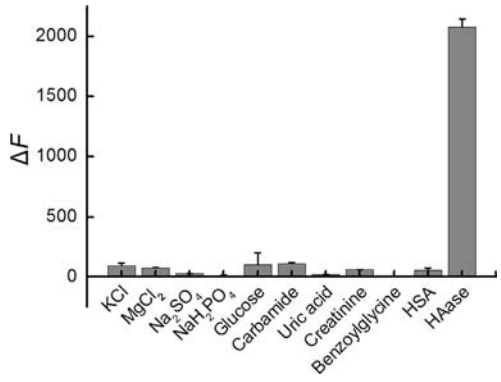

Fig. 6. Enhanced fluorescence intensity (ΔF) of the FITC–HA–AuNPs (60 nmol L^{-1}) to various substances: KCl (15 mM), $MgCl_2$ (2.5 mM), Na_2SO_4 (100 mM), NaH_2PO_4 (100 mM), Glucose glucose (10 mM), carbamide (150 mM)), uric acid (10 mM), creatinine (10 mM), benzoylglycine (10 mM), HSA (1000 μg mL^{-1}), HAase (50 U mL^{-1}). ΔF is the difference of fluorescence intensity of the FITC–HA–AuNPs in the presence and absence of a substance.

proteins, and is the commonly used clinical specimen for HAase detection [20,45,46], the selectivity detection of HAase from the interference of other molecules is critical for the evaluation of the FITC–HA–AuNPs nanoprobes. To exclude the interference of these components, we tested the effects of several typical substances on the FITC–HA–AuNPs nanoprobes with the same procedure as above for HAase. The results in Fig. 6 show that non-protein substances (*e.g.*, KCl; $MgCl_2$; carbamide; uric acid; creatinine; benzoylglycine) had no obvious effect even with micromole level concentrations. In addition, proteins in human urine, *e.g.*, HSA also had no significant effect eventhough its abundance is much higher than that of HAase used above (50 U mL^{-1}) [47]. This study demonstrated that the FITC–HA–AuNPs nanoprobes had a good selectivity for HAase, which makes our FITC–HA–AuNP an excellent candidate for HAase detection in complex specimens in clinical diagnosis.

3.6. Reproducibility of FITC–HA–AuNPs nanoprobes

Reproducibility is critical for clinical applications. To investigate the reproducibility of the FITC–HA–AuNPs nanoprobes for HAase detection, we analyzed intra- and inter-assay variations (Table S1). Inter-assay analysis was done by determining HAase in two specimens of different amounts of HAase (1.25 U mL^{-1} and 50 U mL^{-1}) with different batches of the FITC–HA–AuNPs nanoprobes. And the relative standard deviations (RSDs) were in the range of 3.10–6.57%. Intra-assay analysis was carried out by determining HAase in three identical batches of specimens with two different concentrations (1.25 U mL^{-1} and 50 U mL^{-1}). The RSDs of the intra-assay were in the range of 0.95–1.10%. Thus, both the intra- and inter-assay analyses revealed a high level of reproducibility when using FITC–HA–AuNPs nanoprobes to measure HAase in aqueous specimens.

3.7. Determination of HAase in urine specimens with FITC–HA–AuNPs nanoprobes

The above study demonstrated the validity and specificity of the FITC–HA–AuNPs nanoprobes for HAase analysis in buffer system. Furthermore, the FITC–HA–AuNPs nanoprobes were used to detect HAase in clinical specimens (urine from patient with bladder cancer) to determine their practical value. Prior to analysis, the urine specimens from 20 bladder carcinoma patients with grade from 1, 2 to 3 (Table S2) were diluted to ensure that the concentrations of HAase were in the linear range of the assay as done above. Table 1 shows that the concentrations of HAase in urine specimens from patients with bladder carcinoma were between 53.19 and 170.97 U mL^{-1}, and the mean levels of HAase increased by several folds over the group of normal healthy people (2.96–21.98 U mL^{-1}), which was in agreement with the previous findings of HAase level for other bladder carcinoma patients [46,48]. Moreover, it could be found that the level of HAase increased with the increase of the grade of bladder cancer in our study, which showed a similar tendency as the previous study [49]. To determine the recovery efficiency of FITC–HA–AuNPs nanoprobe-based assay for the HAase in urine specimens, 10.0 U mL^{-1} commercial HAase was added to the diluted urine specimen and the total amount of HAase in the specimen was then measured. The results in Table 1 showed that FITC–HA–AuNPs nanoprobe-based assay had recovery efficiency in the range of 92.8–106.9% in different specimens with RSDs in the range of

Table 1
Recovery test of the FITC–HA–AuNPs nanoprobes for HAase in human urine specimens.

Human urine specimens	Numbers	Initial[a] (U mL^{-1})	Added (U mL^{-1})	Found[b] (U mL^{-1})	RSD (%)	Recovery (%)
Normal healthy people	1	2.96	10.0	13.42	2.50	104.6
	2	11.55	10.0	22.92	4.85	103.7
	3	10.87	10.0	20.99	3.02	101.2
	4	21.98	10.0	32.57	2.01	105.9
	5	20.72	10.0	30.01	1.37	92.8
Patients with bladder cancer	1	70.03	10.0	80.36	0.62	103.3
	2	53.19	10.0	63.85	4.10	106.6
	3	115.35	10.0	126.04	0.42	106.9
	4	151.92	10.0	162. 07	0.32	101.5
	5	70.23	10.0	79.63	2.60	94.0
	6	90.67	10.0	94.01	0.51	93.3
	7	106.09	10.0	116.82	4.33	107.3
	8	78.89	10.0	89.38	0.18	104.9
	9	69.67	10.0	79.49	0.25	98.2
	10	99.41	10.0	109.69	2.76	102.8
	11	107.81	10.0	121.22	0.36	102.9
	12	167.86	10.0	177.64	0.07	97.8
	13	170.97	10.0	181.40	0.32	104.3
	14	140.01	10.0	149.77	1.38	97.6
	15	140.07	10.0	150.59	3.14	105.2
	16	151.55	10.0	168.81	2.29	102.6
	17	149.40	10.0	159.71	1.03	103.1
	18	174.12	10.0	184.42	4.19	103.0
	19	145.10	10.0	155.35	1.46	102.5
	20	168.05	10.0	178.44	1.25	103.9

[a] Human urine samples were diluted prior to assay.
[b] The average value of three successive tests of different batches.

0.07–4.85%, demonstrating a high recovery efficiency and accuracy of resultant FITC–HA–AuNPs nanoprobes for the detection of HAase in human urine.

4. Conclusions

In summary, a novel kind of FITC–HA–AuNPs nanoprobes for sensitive, rapid, and accurate analysis of tumor marker (HAase) has been developed. Compared with a similar nanoprobes, the resultant FITC–HA–AuNPs nanoprobes were much easy to prepare and significantly stable under external conditions, and a detection limit as low as 0.63 U mL^{-1} for HAase was achieved using the FITC–HA–AuNPs nanoprobes, with high selectivity even in the presence of other urine ingredients. More importantly, the newly developed FITC–HA–AuNPs nanoprobes are capable of detecting HAase in complex clinical human urine specimens rapidly (within 3 h) and accurately (the recovery efficiency in the range of 92.8–106.9% with RSD $\leq$ 4.85%). According to our understanding, this is the first report demonstrating the application of FITC–HA–AuNPs nanoprobes for HAase detection in clinical urine specimens, showing the exciting potentials of the FITC–HA–AuNPs FRET nanoprobes for clinical diagnosis of HAase-related diseases, such as bladder cancer and so on.

Acknowledgments

This work was supported by the National Natural Science Foundation of China (21005064, 21035005), the Fundamental Research Funds for the Central Universities (XDJK2013B009, XDJK2014A020), the State Key Laboratory of Chemo/Biosensing and Chemometrics, Hunan University (2012009), and the Program for Innovative Research Team in University of Chongqing (2013).

Appendix A. Supporting information

Supplementary data associated with this article can be found in the online version at http://dx.doi.org/10.1016/j.talanta.2014.07.005.

References

[1] B. Zhou, J.A. Weigel, L.A. Fauss, P.H. Weigel, J. Biol. Chem. 275 (2000) 37733–37741.
[2] T. Ahrens, V. Assmann, C. Fieber, C.C. Termeer, P. Herrlich, M. Hofmann, J.C. Simon, J. Investig. Dermatol. 116 (2001) 93–101.
[3] K.Y. Choi, K.H. Min, H.Y. Yoon, K. Kim, J.H. Park, I.C. Kwon, K. Choi, S.Y. Jeong, Biomaterials 32 (2011) 1880–1889.
[4] E.A. Turley, J. Biol. Chem. 277 (2001) 4589–4592.
[5] W. Knudson, G. Chow, C.B. Knudson, Matrix Biol. 21 (2002) 15–23.
[6] K. Meyer, J.W. Palmer, J. Biol. Chem. 107 (1934) 629–634.
[7] C. Kolliopoulos, D. Bounias, H. Bouga, D. Kyriakopoulou, M. Stavropoulos, D.H. Vynios, J. Pharm. Biomed. 83 (2013) 299–304.
[8] S. Eissa, H. Shehata, A. Mansour, M. Esmat, O. El-Ahmady, Med. Oncol. 29 (2012) 3345–3351.
[9] J.T. Posey, M.S. Soloway, S. Ekici, M. Sofer, F. Civantos, R.C. Duncan, V.B. Lokeshwar, Cancer Res. 63 (2002) 2638–2644.
[10] A. Dorfman, M.L. Ott, J. Biol. Chem. 172 (1948) 367–375.
[11] M.R. Magalhaes, N.J. da Silva, C.J. Ulhoa, Toxicon 51 (2008) 1060–1067.
[12] K.P. Vercruysse, A.R. Lauwers, J.M. Demeester, Biochem. J. 306 (1995) 153–160.
[13] B. Steiner, D. Cruce, Anal. Biochem. 200 (1992) 405–410.
[14] M. Stern, R. Stern, Matrix Biol. 12 (1992) 397–403.
[15] B. Delpech, P. Bertrand, C. Maingonnat, N. Girard, C. Chauzy, Anal. Biochem. 229 (1995) 35–41.
[16] S. Pattanaargson, J. Roboz, Toxicon 34 (1996) 1107–1117.
[17] J. Matysiak, P. Derezinski, B. Urbaniak, A. Klupczynska, A. Zalewska, Z.J. Kokot, Biomed. Chromatogr. 27 (2013) 1070–1078.
[18] I. Muckenschnabel, C. Bernhardt, T. Spruss, B. Dietl, A. Buschauer, Cancer Lett. 131 (1998) 13–20.
[19] J.W. Kim, J.H. Kim, S.J. Chung, B.H. Chung, Analyst 134 (2009) 1291–1293.
[20] A.I. Nossier, S. Eissa, M.F. Ismail, M.A. Hamdy, H.M.E.-S. Azzazy, Biosens. Bioelectron. 54 (2014) 7–14.
[21] B. Leslie, C. Benchetrita, L. Sham, B. Pahujaa, D. Ernest, B. Graya, D. Ronald, B. Edstroma, Anal. Biochem. 79 (1977) 431–437.
[22] R.M. Rich, M. Mummert, Z. Foldes-Papp, Z. Gryczynski, J. Borejdo, I. Gryczynski, R. Fudala, J. Photochem. Photobiol. B 116 (2012) 7–12.
[23] R. Fudala, M.E. Mummert, Z. Gryczynski, L. Gryczynski, J. Photochem. Photobiol. B 104 (2011) 473–477.
[24] T. Takahashi, M. Ikegami-Kawai, R. Okuda, K. Suzuki, Anal. Biochem. 322 (2003) 257–263.
[25] J. Mullegger, S. Reitinger, G. Lepperdinger, Anal. Biochem. 293 (2001) 291–293.
[26] K.S. Girish, K. Kemparaju, Life Sci. 80 (2007) 1921–1943.
[27] R.M. Clegg, Curr. Opin. Biotechnol. 6 (1995) 103–110.
[28] M.O. Noor, U.J. Krull, Anal. Chem. 85 (2013) 7502–7511.
[29] W.L. Wei, C. Xu, J.S. Ren, B.L. Xu, X.G. Qu, Chem. Commun. 48 (2012) 1284–1286.
[30] J. Chen, Y. Huang, S.L. Zhao, X. Lu, J.N. Tian, Analyst 137 (2012) 5885–5890.
[31] J.P. Tian, H.M. Zhao, M. Liu, Y.Q. Chen, X. Quan, Anal. Chim. Acta 723 (2012) 83–87.
[32] Y. Wang, Z.H. Li, D.H. Hu, C.T. Lin, J.H. Li, Y.H. Lin, J. Am. Chem. Soc. 132 (2010) 9274–9276.
[33] E. Song, D. Cheng, Y. Song, M. Jiang, J. Yu, Y. Wang, Biosens. Bioelectron. 47 (2013) 445–450.
[34] K.E. Sapsford, L. Berti, I.L. Medintz, Angew. Chem. Int. Ed. 45 (2006) 4562–4588.
[35] M.C. Daniel, D. Astruc, Chem. Rev. 104 (2004) 293–346.
[36] L. Dykman, N. Khlebtsov, Chem. Soc. Rev. 41 (2012) 2256–2282.
[37] A.D. Quach, G. Crivat, M.A. Tarr, Z. Rosenzweig, J. Am. Chem. Soc. 133 (2011) 2028–2030.
[38] P.C. Ray, A.K. Singh, D. Senapati, Z. Fan, Chem. Soc. Rev. 41 (2012) 3193–3209.
[39] X.C. Lu, X. Dong, K.Y. Zhang, X.W. Han, X. Fang, Y.Z. Zhang, Analyst 138 (2013) 642–650.
[40] H. Lee, K. Lee, I.K. Kim, T.G. Park, Biomaterials 29 (2008) 4709–4718.
[41] E. Song, J. Li, H. Wei, Y. Song, Anal. Methods 4 (2012) 1199.
[42] K.C. Grabar, R.G. Freeman, M.B. Hommer, M.J. Natan, Anal. Chem. 67 (1995) 735–743.
[43] J.I. Choi, J.K. Kim, J.H. Kim, D.K. Kweon, J.W. Lee, Carbohyd. Polym. 79 (2010) 1080–1085.
[44] B.N. Khlebtsov, N.G. Khlebtsov, Colloid J. 73 (2011) 118–127.
[45] V.B. Lokeshwar, W.H. Cerwinka, B.L. Lokeshwar, Cancer Res. 65 (2005) 2243–2250.
[46] V.B. Lokeshwar, C. Obek, H.T. Pham, D. Wei, M.J. Young, R.C. Duncan, M. S. Soloway, N.L. Block, J. Urol. 163 (2000) 348–356.
[47] W.L. Roberts, W.E. Owen, Am. J. Clin. Pathol. 124 (2005) 219–225.
[48] H. Jamshidian, M. Hashemi, M.R. Nowroozi, M. Ayati, M. Bonyadi, V.N. Tousi, Urol. J. 11 (2014) 1232–1237.
[49] S.H. Hautmann, V.B. Lokeshwar, G.L. Schroeder, F. Civantos, R.C. Duncan, R. Gnann, M.G. Friedrich, M.S. Soloway, J. Urol. 165 (2001) 2068–2074.